Transplantation of acellularized amniotic membrane seeded with adipose-derived mesenchymal stem cells in a rat model of intrauterine adhesion

Chunbo Li
The Obstetrics & Gynecology Hospital of Fudan University
Luopei Guo
The Obstetrics & Gynecology Hospital of Fudan University
Keqin Hua (huakeqinjiaoshou@163.com)
The Obstetrics & Gynecology Hospital of Fudan University

Research Article

Keywords: intrauterine adhesions, stem cells, tissue engineering, regeneration, acellularized amniotic membrane

Posted Date: July 27th, 2022

DOI: https://doi.org/10.21203/rs.3.rs-1458728/v2

Abstract

Background

Intrauterine adhesion (IUA) is characterized by the formation of fibrosis that prevent the regeneration of functional endometrium. Although various clinical approaches have been used to reconstruct the anatomy and promote the restoration of functional endometrium, the high risk of recurrence after surgery remains a major challenge. Application of tissue engineering offers new therapeutic strategies.

Aim

The aim of this study was to investigate the role of acellularized amniotic membrane (AAM) loaded with adipose-derived mesenchymal stem cells (ADSCs) in reducing IUA, and promoting the regeneration of damaged endometrium.

Methods

96 female Spargue-Dawley (SD) rats were randomly divided into four groups: sham operation group, IUA model group, experimental group treated with AAM, and experimental group treated with AAM loaded with ADSCs. Histological and immunohistochemical analysis were performed on 3, 7, and 14 days after surgery to evaluate the degree of uterine fibrosis and regeneration of injured endometrium. RNA sequencing and real-time polymerase chain reaction (RT-PCR) were used to explore the potential mechanism by which ADSCs modulated immune response and promoted endometrial regeneration.

Results

At 14 days after surgery, the endometrial thickening, the number of glands and the degree of reduced fibrosis in the ADSCs/AAM was higher than those in AAM group, and similar to sham group. RNA sequencing analysis showed that ADSCs can modulate local immune responses, and promote the formation of functional endometrium. Meanwhile, we found that transplantation of ADSCs significantly decreased the expression of pro-inflammatory cytokines expression (TNF-α and IL-1β), and increased the expression of anti-inflammatory cytokines (bFGF, and IL-6).

Conclusion

Our results demonstrated that AAM loaded with ADSCs can promote the regeneration of injured endometrium and reduce fibrosis formation. Meanwhile, ADSCs also regulated the immune microenvironment, which is beneficial to functional endometrial regeneration.

Introduction

Intrauterine adhesion (IUA) is characterized by the formation of fibrosis, with adhesion tissue partially or completely obliterating the uterine cavity as a result of various damage to the basal endometrial layer [1, 2]. It often leads to menstrual abnormalities, secondary infertility and recurrent miscarriage, which is a serious reproductive health problem [3]. Although various clinical approaches have been used to reconstruct the anatomy of the uterine cavity and promote the restoration of a functional endometrium, including hysteroscopic adhesiolysis, hormonal treatment or the placement of barriers (e.g. barrier gels, intrauterine device), the high risk of re-adhesion after resection remains a major challenge [4]. In order to prevent the recurrence of adhesions and promote the regeneration of the endometrium, the application of tissue engineering provides a new therapeutic strategy [5]. The acellularized amniotic membrane (AAM) is a membrane composed of epithelial, basement, and mesenchymal layers [6]. Due to its outstanding advantages of low immunogenicity and high absorbability, AAM has been widely used to repair epithelial defects such as skin, eye, abdominal wall, and peritoneum [7, 8]. Some studies have reported the value of AAM in reducing intrauterine adhesion and promoting endometrial regeneration [7].

In patients with severe IUA, when the basal layer is severely damaged, even though the uterine cavity can be restored by adhesiolysis, the prognosis is still poor due to the failure of functional endometrial regeneration [9]. Endometrial stem cells (ESCs) are considered to be a source of progenitor cells that can differentiate into the endometrium, and also play a key role in the rapid replacement of functional layers [10]. According to previous reports, ESCs can differentiate into endometrial glandular epithelial cells, stromal cells and endothelial cells in vitro [10, 11]. However, ESCs are relatively difficult to obtain because the sterility of the cells must meet high requirements. Therefore, it is important to develop alternative, available, abundant, and immune-privileged cell sources. Adipose-derived mesenchymal stem cells (ADSCs) are precursor cells that have been proved to secrete a variety of bioactive molecules (e.g. growth factors, cytokines and chemokines) [11]. Several studies have also reported that ADSCs can be recruited into the uterus, where they differentiate into endometrial cells and promote angiogenesis, so as to achieve better pregnancy outcomes [12–14]. However, the matter is, that stem cells often migrate elsewhere after implantation due to the lack of a supportive scaffold. Therefore, in order to avoid the loss of ADSCs during IUA treatment, appropriate materials should be used as carriers to provide support for cell transplantation.

In the present study, acellularized amniotic membrane (AAM) is used to as a scaffold to provide support to avoid the spread of ADSCs. The propose of this study was to evaluate the feasibility and effectiveness of acellularized amniotic membrane (AAM) loaded with adipose-derived mesenchymal stem cells (ADSCs) in reducing intrauterine fibrosis, and promoting the regeneration of the injured endometrium, and to explore the potential mechanism of ADSCs regulating immune microenviroment (Fig. 1).

Result

Characteristics of ADSCs, acellularization of amniotic membrane and compounds of ADSCs/AAM

ADSCs obtained from rat inguinal subcutaneous fat were cultured to the third generation. FACS analysis showed that the expression of ADSCs surface markers CD29, CD44 and CD90 was 96.19%, 99.86% and 99.73%, respectively, while the expression of hematopoietic stem cell markers CD11b and CD45 was 0.31% and 0.24% (Figure 2A). Osteogenesis, adipogenic and chondrogenic differentiation were confirmed by alizarin-Red staining, oil red O staining, and toluidine blue staining, respectively (Figure 2B). ADSCs exhibited fibroblast-like morphology (Figure 3A). Fluorescence microscope revealed the shape of ADSCs pre-labeled with the fluorescent dye DiI (Figure 3B). AAM exhibited a thin-film structure, which can be easily tailored to various shapes to fill the defect (Figure 2C). Live/dead staining showed that ADSCs could continue to proliferate without apoptosis (Figure 3D1 and 3D2). SEM showed that there were only collagen fibers on AAM (Figure 3E1 and 3E2), while abundant ECM deposition were observed on ADSCs/AAM compounds (Figure 3F1 and 3F2).

Regeneration of injured endometrium

To evaluate the value of ADSCs and AAM in treating IUA, we applied ADSCs/AAM or single AAM to rat IUA models. In the sham operation group, the endometrial surface was covered by highly columnar epithelial cells. In the ADSCs/AAM group, on day 14 after operation, HE staining showed that the endometrial layer was structurally intact with normal epithelial cells, similar to the sham operation group. Endometrial thickness and number of glands were higher than those in the AAM group. However, in the IUA group, the endometrial layer and myometrium of the uterine cavity were completely destroyed (Figures 4 and 5).

To assess the extent of endometrial fibrosis in injured endometrium in the IUA rat model, we performed Masson staining of collagen fibers. In the sham group, there was almost no collagen deposition in the endometrial stroma. There was a significant increase of the collagen deposition in the IUA group, compared to the sham operation group. However, the rate of endometrial fibrosis was significantly lower in the ADSCs/AAM group, compared to that in the IUA group on day 14 postoperatively (Figure 4 and 5).

Then, we performed immuno-expression of CD31, VEGF, vimentin and E-cadherin in all groups on day 14 postoperatively (Figure 6). CD31 is an marker of endothelial cell presented in stroma, and can be performed to measure the microvascular density. VEGF is a well-known angiogenic factor presented in the cytoplasm, and is essential for neovascularization. Our results showed that the microvascular density in the ADSCs/AAM group was significantly higher than that in the AAM group, similar to sham operation group. The administration of ADSCs, resulted in slightly higher levels of VEGF, similar to the expression of VEGF in the sham group. Vimentin is a marker protein for stromal cells and is mainly expressed in the cytoplasm of endometrial stromal cells. Compared with the AAM group, vimentin expression was significantly higher in the ADSCs/AAM group, similar to the sham operation group. E-cadherin is a transmembrane protein expressed in epithelial cells, and plays an important role in maintaining the stability of epithelial cells. The expression of E-cadherin was significantly higher in the ADSCs/AAM group than the AAM group (Figure 6).

Finally, we also tested 24 IUA models in 12 rats for pregnancy at 4 weeks after transplantation with or without ADSCs/AAM (Figure 7A). In the sham operation group, 4 uteri conceived (66.7%), while none of

the uteri in the IUA group. In the ADSCs/AAM group, although 3 uterine conceived (50%), the average number of embryos was 1-2 embryos in each uterus, compared to 3-4 embryos in the Sham group (Figure 7B). In contrast, ADSCs/AAM led to an improved trend of fertility recovery, with a pregnancy rate of 50% and 1 ± 2 gestational embryos.

The regulating function of stem cell on inflammatory response

To further explore the regulating mechanism of ADSCs during the endometrial repair, we performed RNA sequencing of uterine tissue at 3 days and 14 days post-operatively. Our results exhibited high expression levels of COL4A1, MSN and HMOX1 in the IUA group at 3 days post-operatively (Figure 8A) and GO analysis showed highly enrichment of endothelium development, lymphangiogenesis and leukocyte migration (Figure 8C). At 14 days after surgery, IUA group showed high COL3A1, COL1A1 and ACTG2 expression, and GO analysis showed high enrichment of extracellular matrix organization, cell-substrate adhesion, endodermal cell differentiation and leukocyte migration. These results indicated that the formation of stable fibrous tissue covered the damaged endometrium. We then evaluated the effect of ADSCs on the formation of fibrosis and endometrial regeneration. Not surprisingly, at 3 days and 14 days after surgery, the ADSCs/AAM group exhibited high expression levels of SPP1, LYZ2, APOE and CTSB compared with that in the sham group (Figure 8B). In early phase, GO analysis showed high enrichment of antigen processing, leukocyte chemotaxis, phagocytosis, neutrophil activation and endocytosis (Figure 8D), indicating that ADSCs could play an immunomodulatory role. In late phase (at 14 days after surgery), GO analysis revealed normal functional enrichment, including ribosome, protein targeting and RNA catabolic process in ADSCs/AAM group (Figure 8D).

Then, we evaluated the expression of inflammatory cytokines (bFGF, IL-1β, IL-6, and TNF-α1) (Figure 9). Our results showed that the expression of anti-inflammatory cytokines, such as bFGF and IL-6, were significantly increased in the ADSCs/AAM group at day 3 and 7 postoperatively compared with the AAM group. Meanwhile, the expression of pro-inflammatory cytokines such as TNF-α and IL-1β was significantly decreased in the ADSCs/AAM group at day 3 and 7 postoperatively compared with the AAM group. However, for both anti-inflammatory and pro-inflammatory cytokines expression at day 14 postoperatively, there was no significant differences between the ADSCs/AAM and AAM groups.

The tracing of stem cell in vivo

ADSCs were labeled with Dil, a flourochrome used to track living cells in vivo. At day 3, 7, and 14 postoperatively, fluorescent microscope revealed that Dil-labeled ADSCs were distributed near the damaged endometrium and had incorporated into the endometrium tissue. The signal attenuated, but was still present at 14 days (Figure 10).

Discussion

IUA usually occurs when the endometrium fails to regenerate and is replaced by fibrotic tissue [15]. Therefore, the ideal treatment must simultaneously prevent fibrosis formation and promote endometrial

regeneration. In this study, we investigated the potential role of AAM loaded with ADSCs in preventing IUA after endometrial injury. Our results indicated that ADSCs/AAM can promote endometrial regeneration by measuring endometrial thickness, gland numbers, and vascular area.

Clinically, hysteroscopic adhesiolysis and intrauterine device (IUD) placement are standard approaches for IUA treatment. However, due to the low biocompatibility of the IUD, it may result in an inflammatory response that prevents functional endometrial regeneration, and even causes intrauterine infection [16]. In this study, we successfully regenerated the endometrium using human AAM. After removal of cellular components, AAM can act as a natural component to enhance cell adhesion, proliferation, and differentiation, making it ideal for regenerative medicine [17]. It is well known that, intrauterine curettage at 2–4 weeks after delivery is most likely to cause scarring and irreversible uterine wall damage. According to our results, we found that AAM gradually degraded and disappeared within 7–14 days after implantation, which happened to play a preventive role against the formation of IUA. Although AAM can effectively prevent fibrotic tissue caused by endometrial injury, it is still a great challenge to promote tissue regeneration, including neovascularization, cell proliferation and endometrial repair.

Basal ESCs are thought to be the source of endometrial regeneration, when the endometrium shades and regenerates during each menstrual cycle [18–20]. ESCs are mainly located in the basal layer of the human endometrium, similar to adult mesenchymal stem cells (MSCs) [19]. It is reported that ESCs played an important role in endometrial regeneration [10, 11]. However, the difficulty in obtaining ESCs limits its wide application. Several other sources of MSCs have also been proposed for endometrial regeneration, such as bone marrow mesenchymal stromal cells (BMSCs), menstrual blood–derived mesenchymal stromal cells (mbMSCs) and amniotic tissue-derived mesenchymal stromal cells (AmMSCs) [13, 21, 22]. They all have a strong ability to reduce uterine fibrosis after endometrial injury. In this study, we selected ADSCs as seed cells, because of their easy availability and rapid expansion. In order to maintain a certain number of implanted cells, we transplanted ADSCs/AAM into the uterine cavity, where ADSCs could migrate gradually into lesion. ADSCs/AAM can produce thicker endometrium, more endometrial glands, and lower fibrotic area than single AAM transplantation. Meanwhile, we also found that the expression level of CD31, VEGF, E-cadherin and vimentin in the ADSCs/AAM group were higher than that in single AAM group. These results indicated that the use of ADSCs/AAM can reduce intrauterine fibrosis and achieve functional endometrium recovery.

The formation of fibrosis is believed to be the excessive deposition of ECM, caused by early inflammatory activity and uncontrolled proliferation of fibroblasts [23]. Our RNA sequencing data suggested that IUA was association with immune activation, endothelial cell and epithelial cell development in the early stages, while at later stages, it is highly enriched of cell-matrix adhesion. When implanted with ADSCs/AAM for the repair of endometrial injury, RNA sequencing showed that ADSCs can regulate immune effector process, neutrophil activation and endocytosis, which is beneficial for reducing immune response. According to previous reports, ADSCs can reduce the expression of pro-inflammatory cytokines, such as IL-1β, TNF-α and IL-8, and increase the expression of anti-inflammatory cytokines, such as IL-6 and IL-10 [24–25]. ADSCs can also inhibit collagen overproduction by regulating inflammatory cytokines

[26]. Our results indicated that ADSCs could up-regulate the expression of anti-inflammatory cytokines (IL-6, and bFGF), and down-regulate the expression of pro-inflammatory cytokines (IL-1 β, and TNFα) at 3 and 7 days after surgery. However, there was no significant differences in all inflammatory factors between the ADSCs/AAM and AAM group at 14 days after surgery, suggesting that ADSCs played a role in suppressing the inflammatory response at an early stage. These phenomena partially explained the mechanism by which ADSCs can maintain a relatively mild immune microenvironment. It is very beneficial for the regeneration of endometrium and the recovery of function.

A particular strength of this study is the high-precision scraping of the depth of the endometrial layer, which is essential for assessing the regenerative capacity of ADSCs in the IUA model. However, our study has some limitations. According to our pregnancy test, the miscarriage rates were high in both the sham group and ADSCs/AAM groups. Severely damaged endometrium may also increase the local inflammatory response and lead to embryo implantation failure. In addition, multiple surgeries and possible ovarian damage are detrimental factors for conception and pregnancy in rats. In addition, the appropriate timing of endometrial repair to obtain high pregnancy rates needs to be explored, which will be carried out in our subsequent studies. More importantly, studies with large samples should be performed to assess pregnancy outcomes.

In conclusion, our findings suggested that AAM loaded with ADSCs can effectively prevent fibrosis formation and promote endometrial regeneration. Although the exact mechanism by which ADSCs in treating IUA remained unclear, our study confirmed that ADSCs can regulate the local immune microenvironment by promoting the secretion of anti-inflammatory factors and inhibiting the secretion of pro-inflammatory factors.

Method

Animals

Ninety-six female Sprague-Dawley (SD) rats weighting 220-240 g were purchased from Silaike Corporation (Shanghai, China). The protocol was approved by the Institutional Review Board and the Ethics Committee of our hospital (number: 2021JS-017). All animal experiments were approved by the Institutional Animal Care and Use Committee of Fudan University, Shanghai, China.

Culture, identification and multilineage differentiation of ADSCs

Rat subcutaneous inguinal fat was collected, chopped manually and digested with equal amounts of PBS, supplemented with 0.075% type I collagenase (Washington Biochemical Corp, USA), and then gentle shaped at 37 ℃ for 60 minutes. After enzyme neutralization, the digested tissue was centrifuged at 2000 g for 10 min and filtered through double-layer gauze to remove large debris. The pellets were resuspended in LG-MEM containing 10% FBS, 100 ug/ml streptomycin and 100 U/ml penicillin solution and plated in 100 mm culture dishes (Falcon, USA). After reaching 70-80% confluency, the cells were passed on to the next generation for further experiments. ADSCs were identified by the cell surface antigens CD45, CD90,

CD11, CD44, and CD29, using flow cytometry assays. The multi-lineage differentiation potential of ADSCs was examined by adipogenic, osteogenic and chondrogenic differentiation assays. Adipogenesis was induced by adipogenic induction medium (Gibco) for 14 days and intracellular lipid accumulation was confirmed by Oil red O staining. Osteogenesis was induced by osteogenic induction medium (Gibco) for 21 days and calcium deposition was shown by alizarin red staining. Chondrogenic differentiation was induced with chondrogenic induction medium (Gibco) for 28 days and identified by toluidine blue staining.

Preparation of human AAM

After obtaining approval of ethics committee of our hospital for the use of human amniotic membrane, fresh human amniotic membrane (AM) was obtained from healthy patients under sterile conditions. The preparation of AAM was based on the report of Koizumi et al. Briefly, fresh AM was mechanically separated from the chorionic membrane. After washing three times with 0.9% NaCl solution, AM was incubated with 0.02% ethylenediaminetetraacetic acid (EDTA) solution at 37 °C for 2 h, with continuous agitation for decellularization. Then, the cellular debris was washed with PBS for three times to remove remaining cellular debris.

The construction of ADSCs/AAM compounds

Before implantation, AAM was cut into 2 × 0.5 cm pieces and soaked in normal saline for 10 min. ADSCs at passage 3 were resuspended in the culture medium at a density of 5×10^5/ml. 100 ul of cell suspension were evenly seeded in AAM to infiltrate the cell surface. After cells were incubated at 37 ℃ for 4 h to allow cells adhere to the membrane, growth medium was added to continue the incubation. After 24 h of incubation, the ADSCs/AAM constructs were transferred to new wells for subsequent in vitro culture.

Scanning electron microscopy (SEM)

The deposition of ADSCs on AAM was examined by scanning electron microscopy 1 week after implantation. Samples were then mounted, sputter-coated with gold, and viewed by SEM to observe adhesion and ECM deposition under the surface of AAM.

Live/dead staining

On days 3 and 7 post-implantation, **t**he viability of ADSCs on AAM was evaluated using a live/dead cell staining kit (Biovision, USA). Briefly, ADSCs/AAM constructs were washed with PBS and incubated in assay reagents (2 uM calcein AM and 4 uM ethidium homodimer-1) for 15 min. Then, stained live and dead cells were detected by confocal laser microscopy with a band-pass filter (FITC and rhodamine). Live cells fluoresced green, while the nuclei of dead cells were stained red.

Surgical procedure

The rat IUA model was established using the mechanical injury method [27]. Briefly, rats were anesthetized with 300 mg/kg 10% chloral hydrate and the abdominal cavity was open after iodophor disinfection. Then, the uterus was slowly pick out and incised 2 cm from the upper one-third of the upper uterus. The endometrial tissue was then scraped to the depth of the muscular layer. In the ADSCs/AAM group, constructs were introduced to cover the damage area. In the AAM group, a AAM alone was placed at the lesion of the uterine. In the IUA group, the lesion was sutured directly to achieve self-healing. In the sham operation group, the uterus was exposed to air for 20 min after opening the abdomen. Finally, the uterus was closed with 6–0 absorbable suture intermittently. After washing the abdominal cavity with saline, the rectus fascia and skin were sutured with 4–0 silk suture. At day 3, 7, and 14 after surgery (n = 12, 12 uteri at each time point), the entire uterus was dissected and sectioned transversely for further evaluation.

Histological examination and immunohistochemical staining

After fixing the uterine tissue with 4% paraformaldehyde and embedding it in paraffin, the samples were cut into 4-6 μm sections for H&E and Masson's trichrome staining. Light microscope was used to counter-view morphological changes. Five areas in each image were selected for counting. Image Pro-Plus 6.0 (IPP 6.0) was applied to analyze endometrial thickness, total number of endometrial glands, and fibrosis area. For immunohistochemistry staining, samples were tested for CD31, GB13063, 1:200, Servicebio, (an indicator of endothelial cells of microvessels), vimentin, ab92547, 1:200, abcam, (a marker of stromal cells), VEGF, ab32152, 1:200, abcam, (a vascular marker) and E-cadherin, sc-8426 1:50, Santa Cruz, (a marker of epithelial cell).

Next-generation RNA sequencing and bioinformatics analysis

Total RNA was extracted from four groups of whole uterus at 3 and 14 days postoperatively using TRIzol according to the manufacturer's protocol (Invitrogen). The Illumina standard kit was used according to the TruSeq RNA SamplePrep Guide (Illumina). Magnetic beads containing oligo (dT) were used to isolate poly(A) mRNA from total RNA. Purified mRNA was then fragmented. Using these short fragments as templates, first-strand complementary DNA (cDNA) was synthesized using random hexamer primers and reverse transcriptase (SuperScript II, Invitrogen). Second-strand cDNA was synthesized using buffer, dNTPs, RNase H and DNA polymerase I. Short double-stranded cDNA fragments were purified using the QIAquick PCR Extraction Kit (Qiagen) and eluted with EB buffer for end repair and the addition of an "A" base. The short fragments were ligated to an Illumina sequencing adapters. DNA fragments of selected size were gel-purified with QIAquick PCR extraction kit (Qiagen) and amplified by PCR. The library was then sequenced on an Illumina HiSeq™ 2000 sequencing machine. The library size was 400 bp, the read length was 116 nt, and the sequencing strategy was paired-end sequencing. Clean reads were used for subsequent analysis and were mapped to the reference genome by TopHat. The gene expression was measured by the number of uniquely mapped fragments per kilobase of exon per million mapped fragments (FPKM). The R package "limma" was used to create differential expression genes. The

Database for Annotation, Visualization, and Integrated Discovery (DAVID) bioinformatics resource was used to annotate gene function and pathway.

RNA isolation and polymerase chain reactions

In order to investigate the regulation effect of ADSCs on inflammatory response, we performed real-time PCR. According to the manufacturer's protocol, RNAprep Micro Kit (TianGen Biotech, Beijing, China) was used to extract total RNA. Total RNA samples were extracted from excised uterine horns with RNAiso Plus (Takara Bio) and dissolved in water treated with diethyl pyrocarbonate. RNA concentrations were quantified using NanoDrop 2000 spectrophotometery (NanoDropTechnologies, 1f in of TGF-β and VEGF in ADsN Thermo Scientific). 2 ug total RNA was reverse-transcribed into cDNA in a 20 ul reverse transcription system with the Primestar extaq cDNA Synthesis Kit (TaKaRa). The reactions were performed and monitored in a T3 thermocycler (Biometra). Real time PCR was performed using a quantitative real time amplification system (MxPro-Mx3000P, Stratagene, La Jolla, CA). SybrGreen PCR MasterMix (Applied Bio-systems, Foster City, CA) was used in each reaction. To compare transcription levels of target genes in different quantities of sample, the quantified cDNA transcript level (cycle threshold) to that of GAPDH was used for normalization of real-time PCR results. Each sample was assayed three times.

Fertility test

The function of the scarred uterine horns was assessed by testing their ability to receive fertilized ova and supporting embryos to the late stage of pregnancy. On day 28 after transplantation, another subset of rats from each group (n = 6, with 12 uterine horns) was mated with fertile male rats. Rats were euthanized 14 days after the presence of the vaginal plugs, and each uterine horn was examined for number, size and weight of fetuses, as well as the site of implantation.

Tracing of ADSCs in vivo

Dil is a nontoxic fluorescent marker of cell membranes that is used to track for implanted cells. ADSCs were labeled with Dil (SigmaeAldrich, St Louis, MO). After washing, stained cells were cultured in sterile phosphate-buffered saline. Dil-labeled ADSCs were then resuspended in the culture medium at a density of 5×10^5/ml and seeded on AAM scaffolds to form ADSCs/AAM compounds, which was implanted in the injured uterine. On day 3, 7, and 14 after implantation, rats were sacrificed, and uterine tissues were collected and frozen at −80 °C. Frozen tissues were continuously cut into 4-μm sections, and the nucleus was stained with DAPI. The samples were then observed by fluorescence microscopy (magnification × 100, Olympus, Tokyo, Japan).

Statistical analysis

All data are reported as means± standard deviation (SD) analyzed by SPSS 20.0. Statistical analysis was performed by Student's t test for comparisons of different groups. A p value less than 0.05 was

considered statistically significant.

Abbreviations

IUA
Intrauterine adhesion
AAM
Acellularized amniotic membrane
ADSCs
adipose-derived mesenchymal stem cells
S-D
Spargue-Dawley
RT-PCR
Real-time polymerase chain reaction
ESCs
Endometrial stem cells
VEGF
Vascular endothelial growth factor
BMSCs
bone marrow mesenchymal stromal cells
mbMSCs
Menstrual blood–derived mesenchymal stromal cells
AmMSCs
Amniotic tissue-derived mesenchymal stromal cells.

Declarations

Acknowledgements

Not appicable

Author Contribution

CB Li and LP Guo contributed equally to this work. CB Li and LP Guo collected the data and did the statistical analysis, CB Li and KQ Hua organized and submitted the manuscript. KQ Hua guided the whole process.

Funding

The Clinical Research Plan of SHDC (SHDC2020CR1045B) to Keqin Hua; Shanghai Municipal Health commission (20194Y0085) to Chunbo Li; The Shanghai “Rising Stars of Medical Tale cvnt” Youth Development Program (SHWSRS2020087) to Chunbo Li.

Data Availability

The authors confirm that the data supporting the findings of this study are available within the article

Ethical Approval and Consent to participate

The protocol was approved by the Institutional Review Board and the Ethics Committee of our hospital.

Consent for publication

Not applicable

Competing interests

All author reported no potential conflict of interest.

Author details

[1]Department of Obstetrics and Gynecology, The Obstetrics & Gynecology Hospital of Fudan University, Shanghai, China.

References

1. Di Spiezio Sardo A, Calagna G, Scognamiglio M, et al. Prevention of intrauterine post-surgical adhesions in hysteroscopy. A systematic review. European journal of obstetrics, gynecology, and reproductive biology. 2016;203:182-92.
2. March CM. Asherman's syndrome. Semin Reprod Med. 2011;29(2):83-94.
3. Guo EJ, Chung JPW, Poon LCY, Li TC. Reproductive outcomes after surgical treatment of asherman syndrome: A systematic review. Best practice & research Clinical obstetrics & gynaecology. 2019;59:98-114.
4. Robinson JK, Colimon LM, Isaacson KB. Postoperative adhesiolysis therapy for intrauterine adhesions (Asherman's syndrome). Fertility and sterility. 2008;90(2):409-14.
5. Salazar CA, Isaacson K, Morris S. A comprehensive review of Asherman's syndrome: causes, symptoms and treatment option. Curr Opin Obstet Gynecol. 2017;29(4):249-56.
6. Gholipourmalekabadi M, Sameni M, Radenkovic D, Mozafari M, Mossahebi-Mohammadi M, Seifalian A. Decellularized human amniotic membrane: how viable is it as a delivery system for human adipose tissue-derived stromal cells? Cell proliferation. 2016;49(1):115-21.
7. Hortensius RA, Harley BA. Naturally derived biomaterials for addressing inflammation in tissue regeneration. Exp Biol Med (Maywood). 2016;241(10):1015-24.

8. Farhadihosseinabadi BF, M, Tayebi T, Jafari A, Biniazan F, Modaresifar K, Moravvej H, et al. Amniotic membrane and its epithelial and mesenchymal stem cells as an appropriate source for skin tissue engineering and regenerative medicine. Artif Cells Nanomed Biotechnol. 2018;46(sup2):431-40.
9. Deans R, Abbott J. Review of intrauterine adhesions. J Minim Invasive Gynecol. 2010;17(5):555-69.
10. Maruyama T, Masuda H, Ono M, Kajitani T, Yoshimura Y. Human uterine stem/progenitor cells: their possible role in uterine physiology and pathology. Reproduction. 2010;140(1):11-22.
11. Nguyen HP, Sprung CN, Gargett CE. Differential expression of Wnt signaling molecules between pre- and postmenopausal endometrial epithelial cells suggests a population of putative epithelial stem/progenitor cells reside in the basalis layer. Endocrinology. 2012;153(6):2870-83.
12. Liu Y, Tal R, Pluchino N, Mamillapalli R, Taylor HS. Systemic administration of bone marrow-derived cells leads to better uterine engraftment than use of uterine-derived cells or local injection. Journal of cellular and molecular medicine. 2018;22(1):67-76.
13. Wang J, Ju B, Pan C, et al. Application of Bone Marrow-Derived Mesenchymal Stem Cells in the Treatment of Intrauterine Adhesions in Rats. Cellular physiology and biochemistry : international journal of experimental cellular physiology, biochemistry, and pharmacology. 2016;39(4):1553-60.
14. Shao X, Ai G, Wang L, et al. Adipose-derived stem cells transplantation improves endometrial injury repair. Zygote. 2019;27(6):1-8.
15. Panayotidis C, Weyers S, Bosteels J, van Herendael B. Intrauterine adhesions (IUA): has there been progress in understanding and treatment over the last 20 years? Gynecological Surgery. 2008;6(10):197-211.
16. Yang JH, Chen CD, Chen SU, Yang YS, Chen MJ. The influence of the location and extent of intrauterine adhesions on recurrence after hysteroscopic adhesiolysis. BJOG. 2016;123(4):618-23.
17. Salah RA, Mohamed IK, El-Badri N. Development of decellularized amniotic membrane as a bioscaffold for bone marrow-derived mesenchymal stem cells: ultrastructural study. J Mol Histol. 2018;49(3):289-301.
18. Azizi R, Aghebati-Maleki L, Nouri M, Marofi F, Negargar S, Yousefi M. Stem cell therapy in Asherman syndrome and thin endometrium: Stem cell- based therapy. Biomedicine & pharmacotherapy = Biomedecine & pharmacotherapie. 2018;102:333-43.
19. Gargett CE, Schwab KE, Deane JA. Endometrial stem/progenitor cells: the first 10 years. Hum Reprod Update. 2016;22(2):137-63.
20. Shamosi A, Mehrabani D, Azami M, et al. Differentiation of human endometrial stem cells into endothelial-like cells on gelatin/chitosan/bioglass nanofibrous scaffolds. Artif Cells Nanomed Biotechnol. 2017;45(1):163-73.
21. Zhao J, Zhang Q, Wang Y, Li Y. Uterine infusion with bone marrow mesenchymal stem cells improves endometrium thickness in a rat model of thin endometrium. Reproductive sciences. 2015;22(2):181-8.
22. Zheng SX, Wang J, Wang XL, Ali A, Wu LM, Liu YS. Feasibility analysis of treating severe intrauterine adhesions by transplanting menstrual blood-derived stem cells. International journal of molecular

medicine. 2018;41(4):2201-12.
23. Bazoobandi S, Tanideh N, Rahmanifar F, et al. Induction of Asherman's Syndrome in Rabbit. J Reprod Infertil. 2016;17(1):10-6.
24. Kapur SK, Katz AJ. Review of the adipose derived stem cell secretome. Biochimie. 2013;95(12):2222-8.
25. Jahandideh S, Khatami S, Eslami Far A, Kadivar M. Anti-inflammatory effects of human embryonic stem cell-derived mesenchymal stem cells secretome preconditioned with diazoxide, trimetazidine and MG-132 on LPS-induced systemic inflammation mouse model. Artif Cells Nanomed Biotechnol. 2018;46(sup2):1178-87.
26. Sukho P, Cohen A, Hesselink JW, Kirpensteijn J, Verseijden F, Bastiaansen-Jenniskens YM. Adipose Tissue-Derived Stem Cell Sheet Application for Tissue Healing In Vivo: A Systematic Review. Tissue Eng Part B Rev. 2018;24(1):37-52.
27. Kuramoto G, Takagi S, Ishitani K, et al. Preventive effect of oral mucosal epithelial cell sheets on intrauterine adhesions. Human reproduction. 2015;30(2):406-16.

Figures

Figure 1

Characteristics of ADSCs. (A) FACS analysis showing the expression of common surface markers of stem cells, CD11b/c, CD29, CD44, CD45 and CD90. (B) These three classic tests of stem cells were present. Osteogenic induction, adipogenic induction and chondrogenic induction of ADSCs.

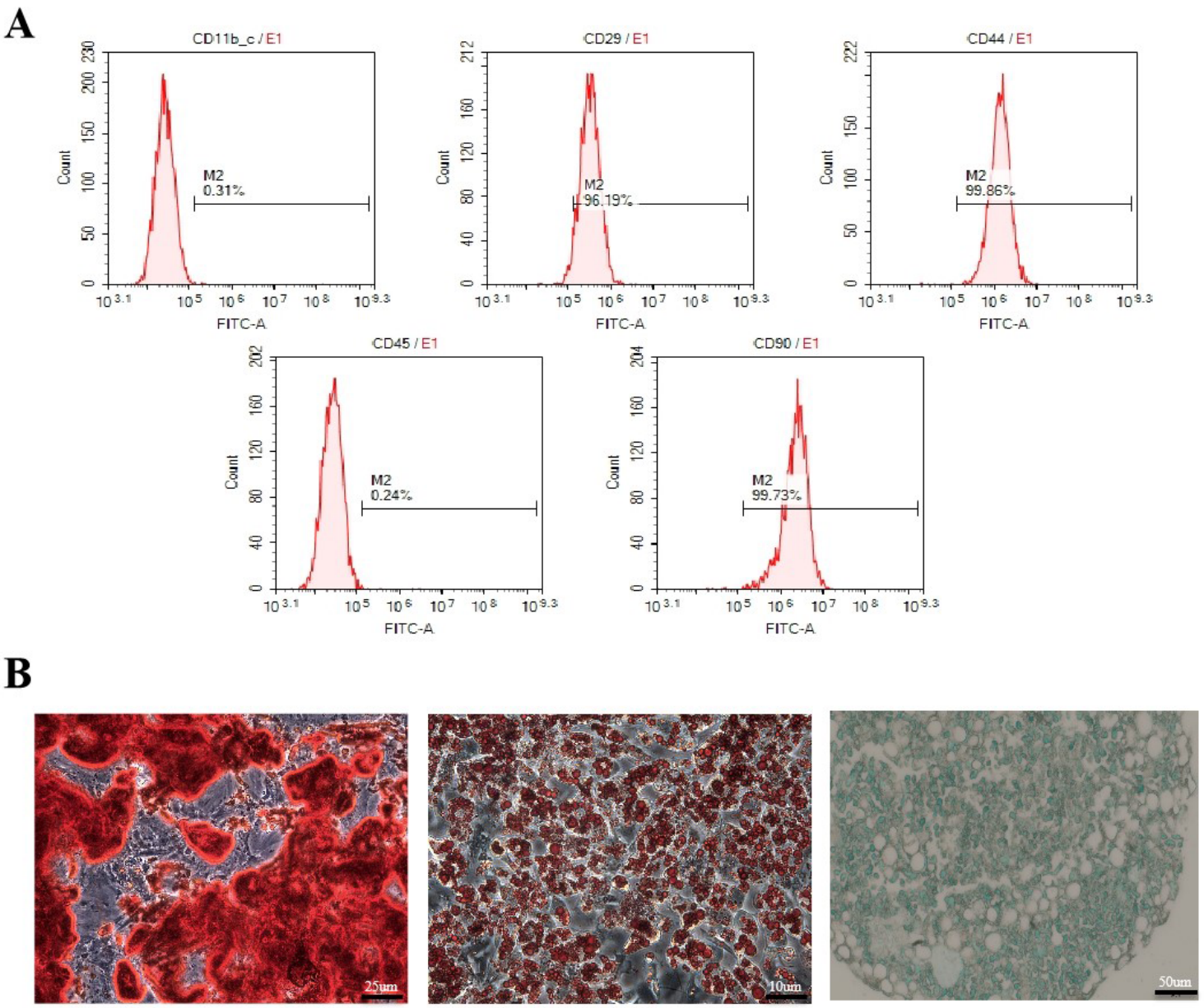

Figure 2

Implantation of adipose derived stem cells (ADSCs) on acellularized amniotic membrane (AAM). (A) Representative image of ADSCs. Scale bar = 500μm；Scale bar = 100μm; (B) ADSCs labeled using Dil． Scale bar = 200μm; (C) Gross view of AAM; (D1, D2) Live/dead staining of ADSCs on the scaffolds after 3 and 14 days; (E1, E2) Representative images of AAM and (F1, F2) AAM implanted with ADSCs by scanning electron microscopy. Scale bar = 200μm.

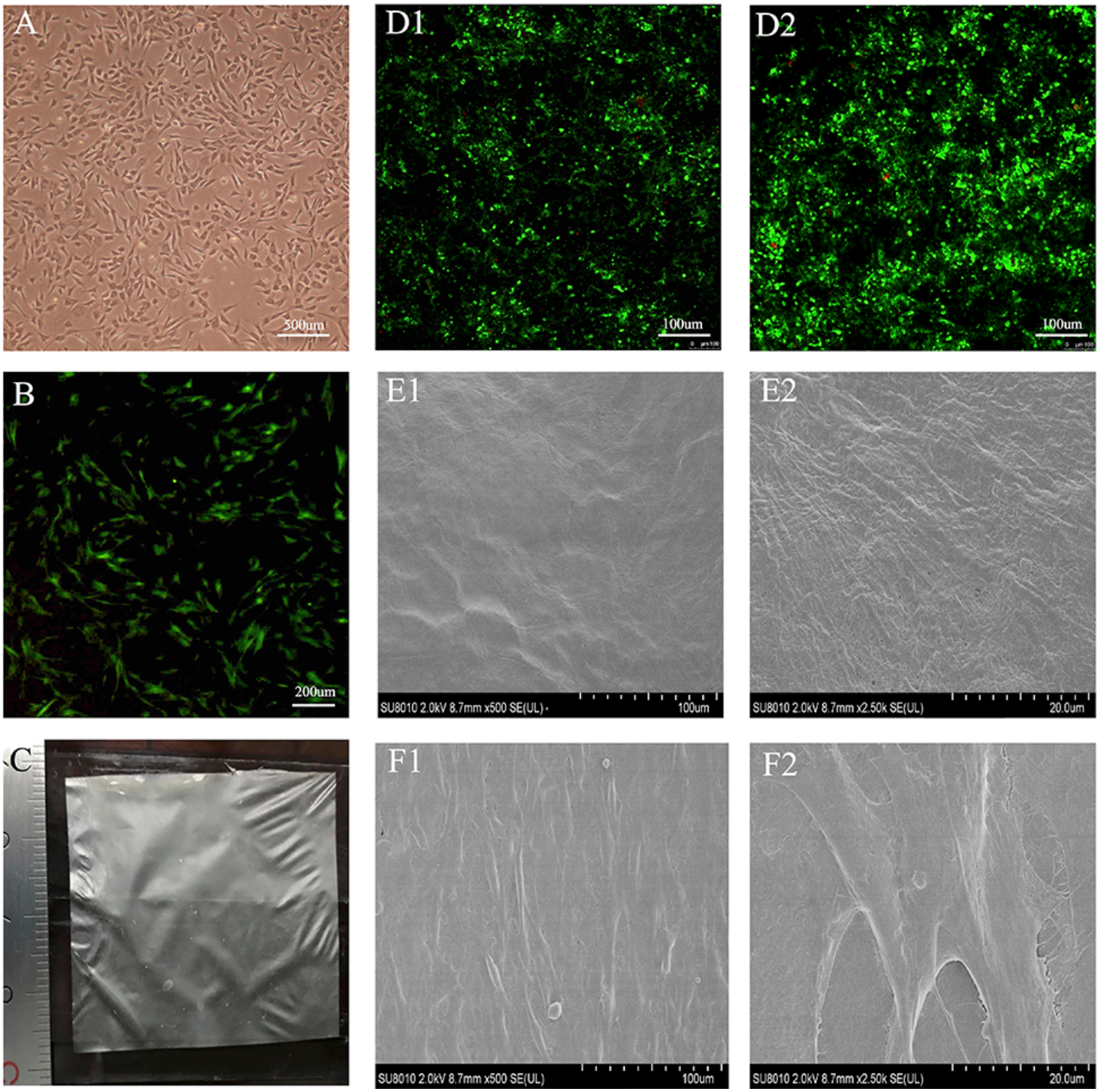

Figure 3

Histopathological characteristics were tested by H&E staining and Masson trichrome staining at 3, 7, and 14 days after surgery in sham, ADSCs/AAM, AAM and IUA group. Scale bar = 200μm. Scale bar = 50μm.

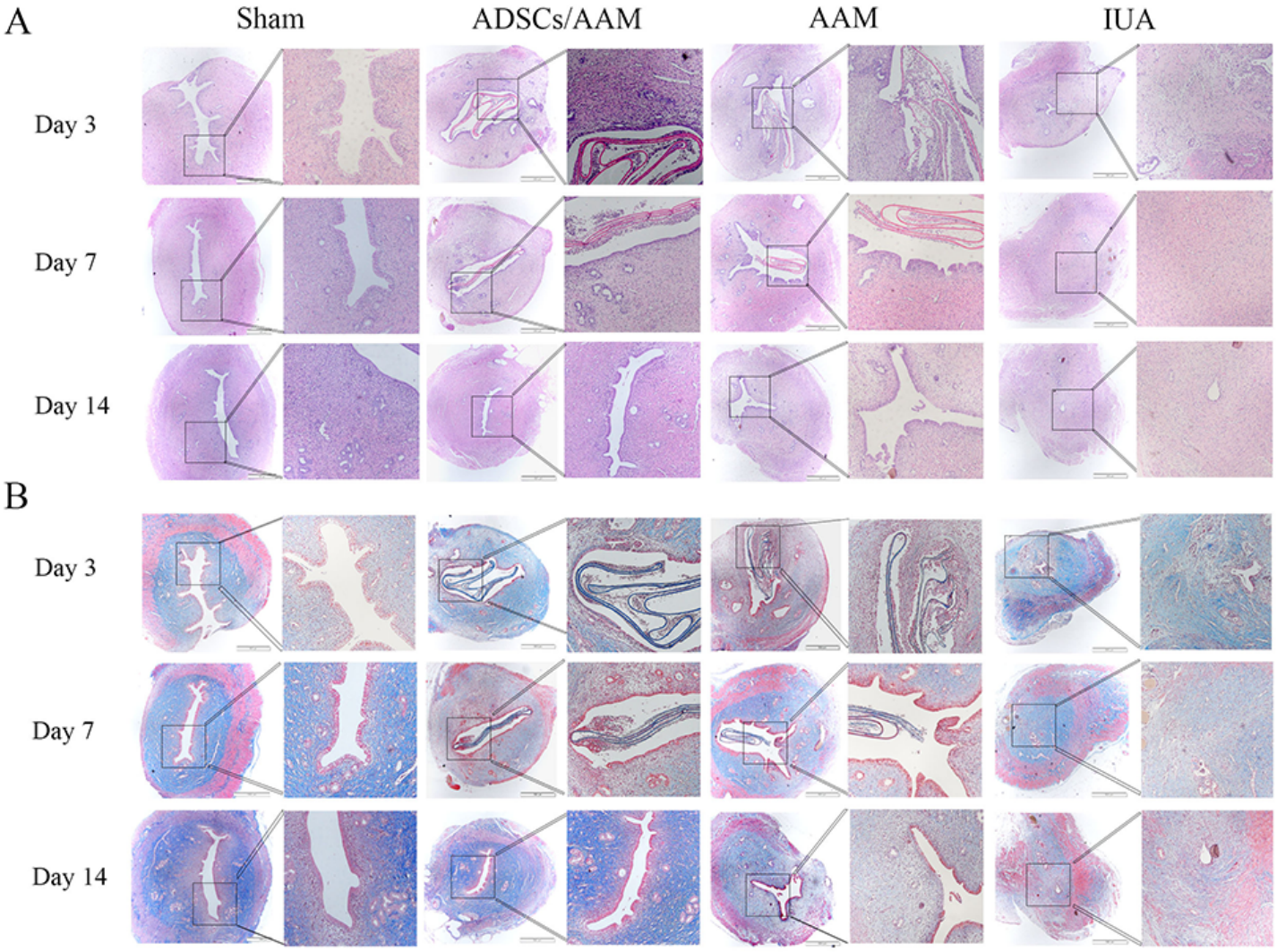

Figure 4

Scoring of thickness of endometrium, number of glands and fibrosis area according to histopathological images at 7, and 14 days postoperatively in the sham, ADSCs/AAM, AAM and IUA group. *p > 0.05 and **p < 0.05. All results are showed as the mean ± SD of three independent experiments.

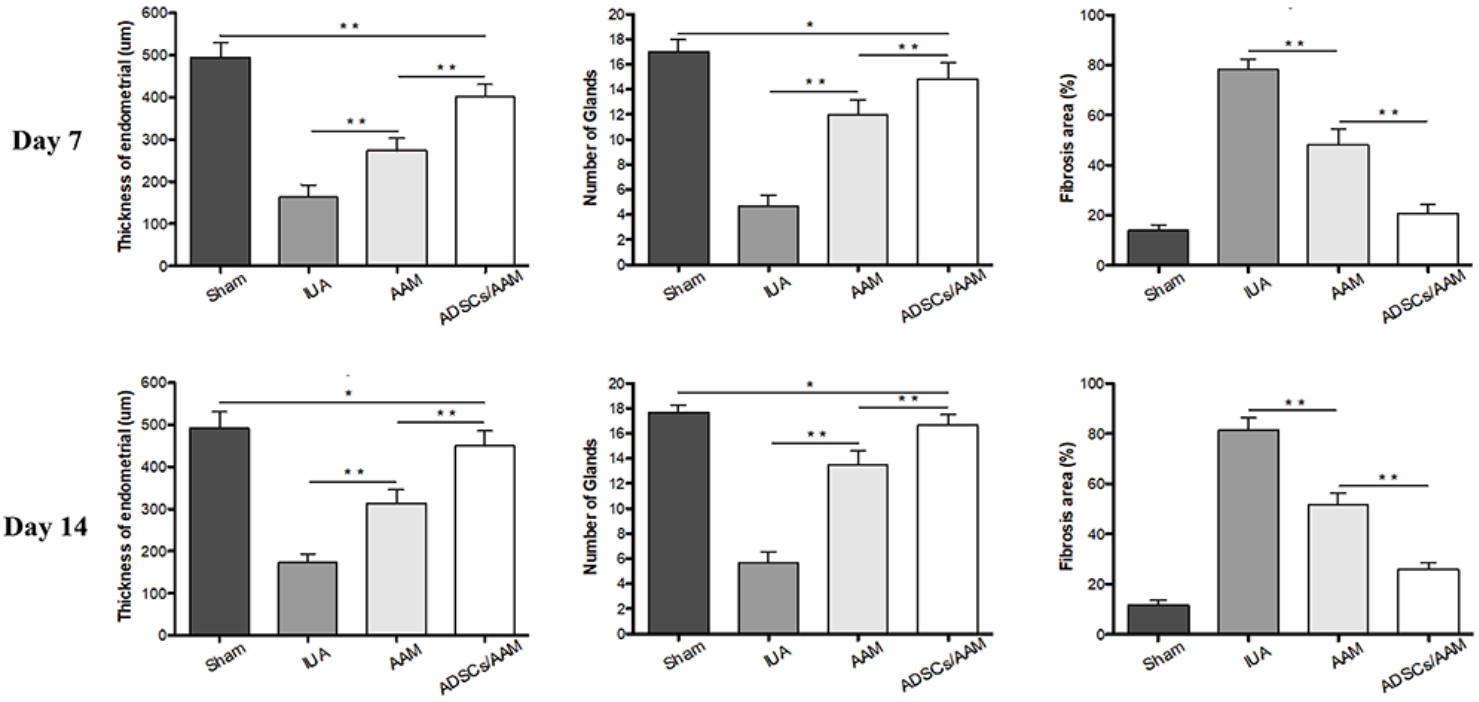

Figure 5

Immunohistochemical staining of CD 31, VEGF, vimentin and E-cadherin at 14 days postoperatively. Scale bar = 50μm.

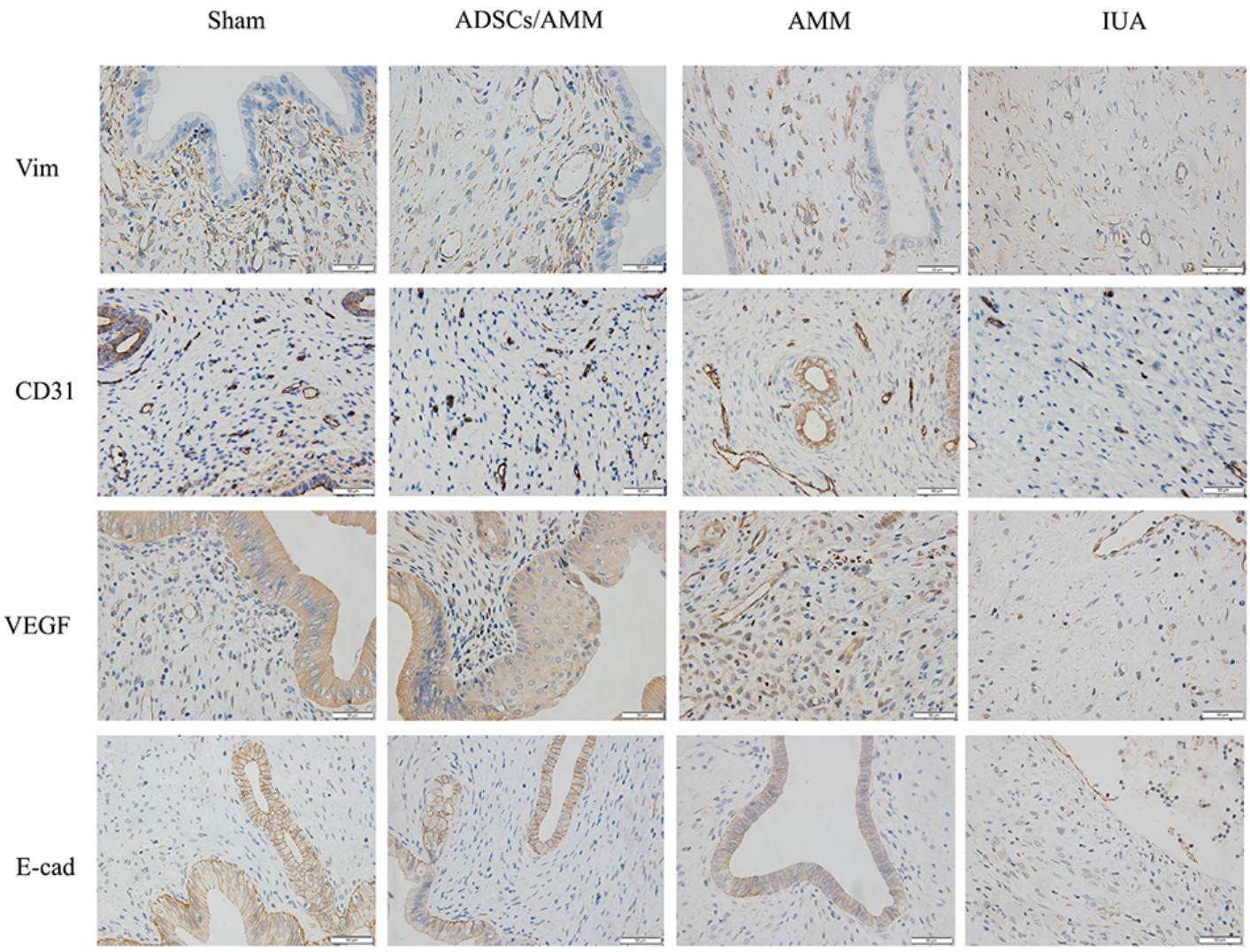

Figure 6

Evaluation of fertility restoration. Representative pictures of uterine horns after 14 days of confirmed mating by vaginal plug (A); Pregnancy rate after 14 days of confirmed mating by vaginal plug (B); Number of gestational sacs after 14 days of confirmed mating by vaginal plug (C).

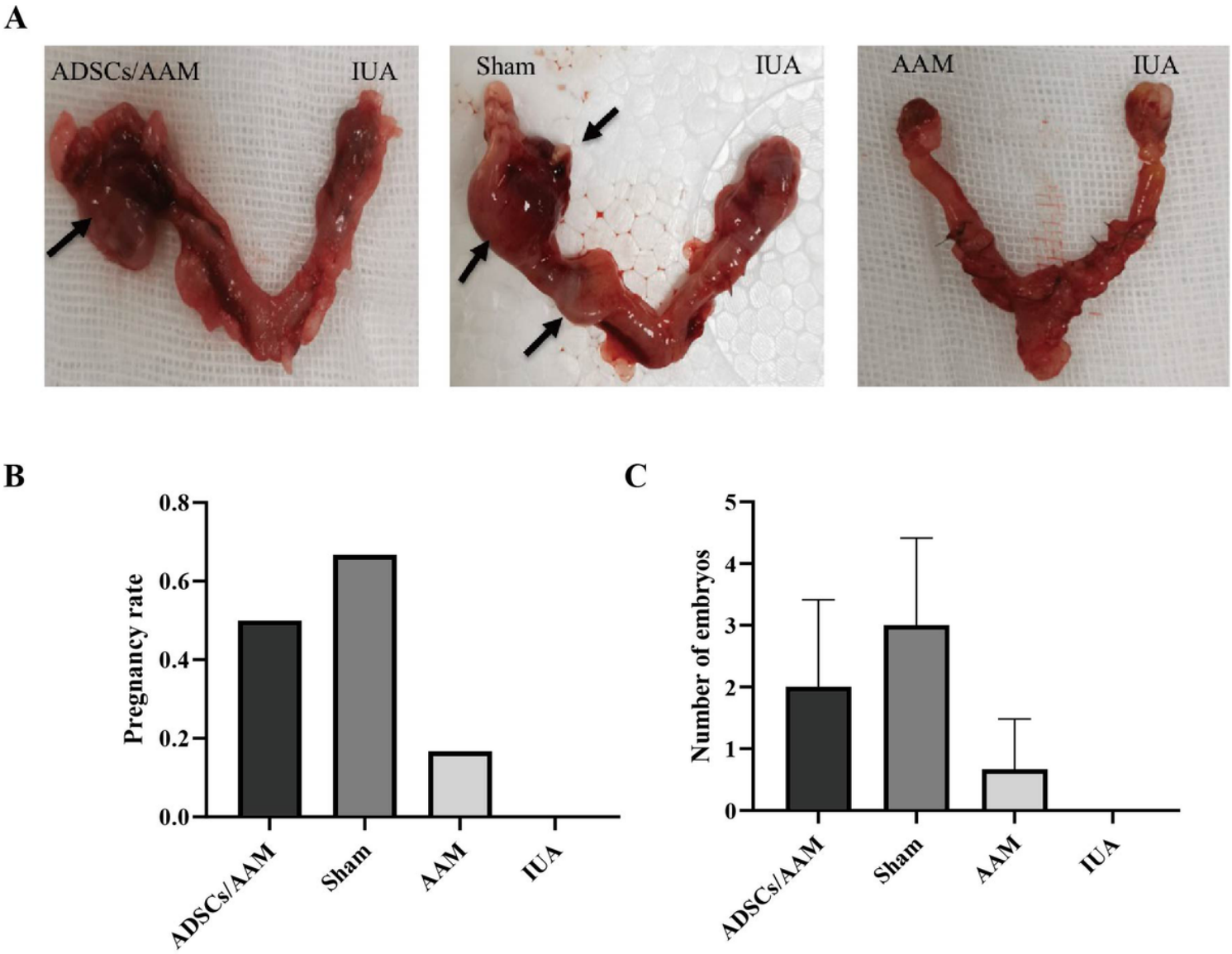

Figure 7

Heatmap of expression profiles of top 10 differently expressed genes (DEGs) between IUA and sham group at 3 days (left) and 14 days (right) after surgery (A); Heatmap of expression profiles of top 10 differently genes between ADSCs/AAM and AAM group at 3 days (left) and 14 days (right) after surgery (B); Comparison of functional enrichment between IUA and sham group at 3 days (left) and 14 days (right) after surgery (C); Comparison of functional enrichment between ADSCs/AAM and AAM group at 3 days (left) and 14 days (right) after surgery (D).

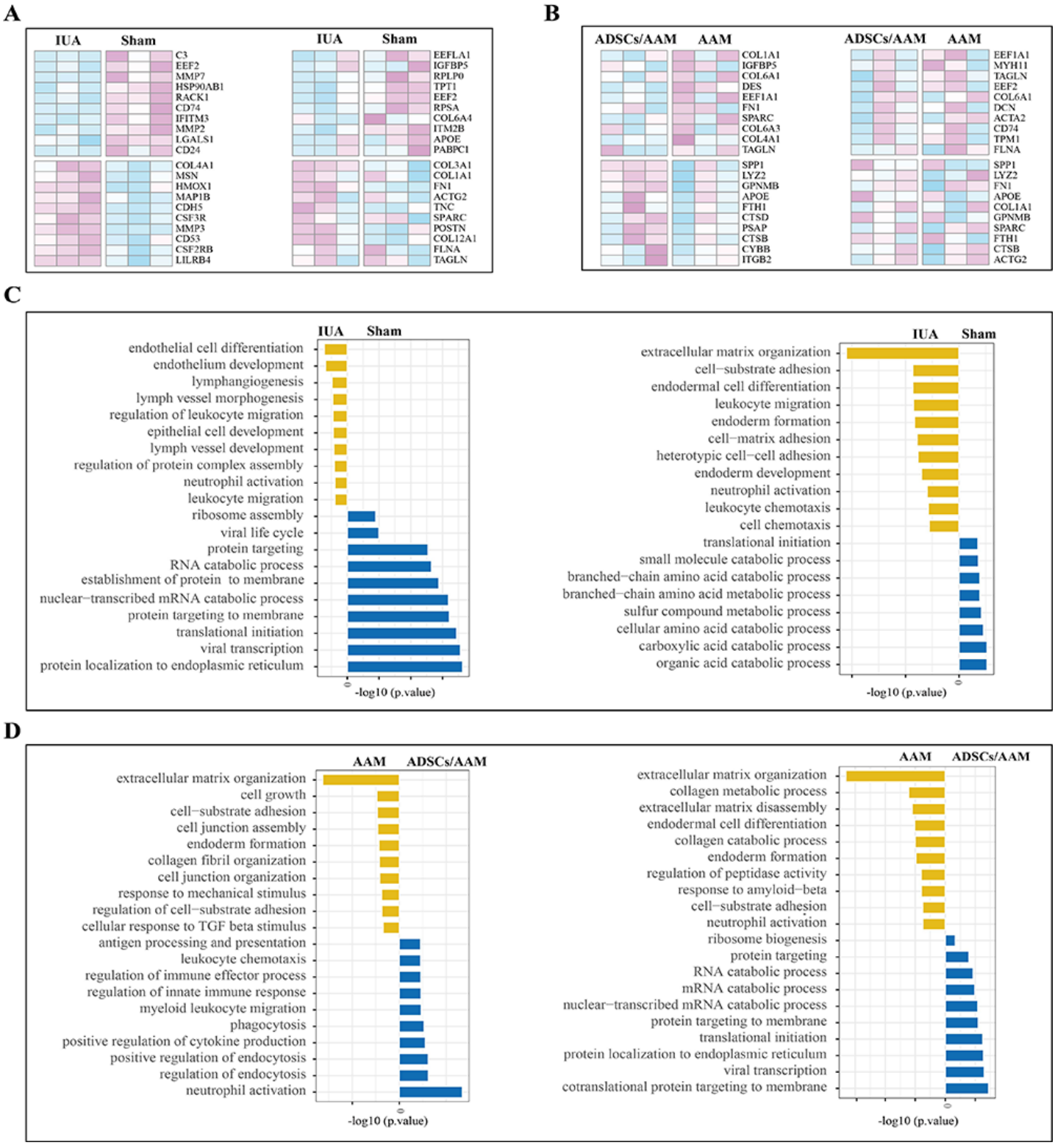

Figure 8

RT-PCR measurements of bFGF, IL-6, TNF-α and IL-1β at 3, 7, and 14 days postoperatively in the sham, ADSCs/AAM, AAM and IUA group. *p > 0.05 and **p < 0.05. All results are showed as the mean ± SD of three independent experiments.

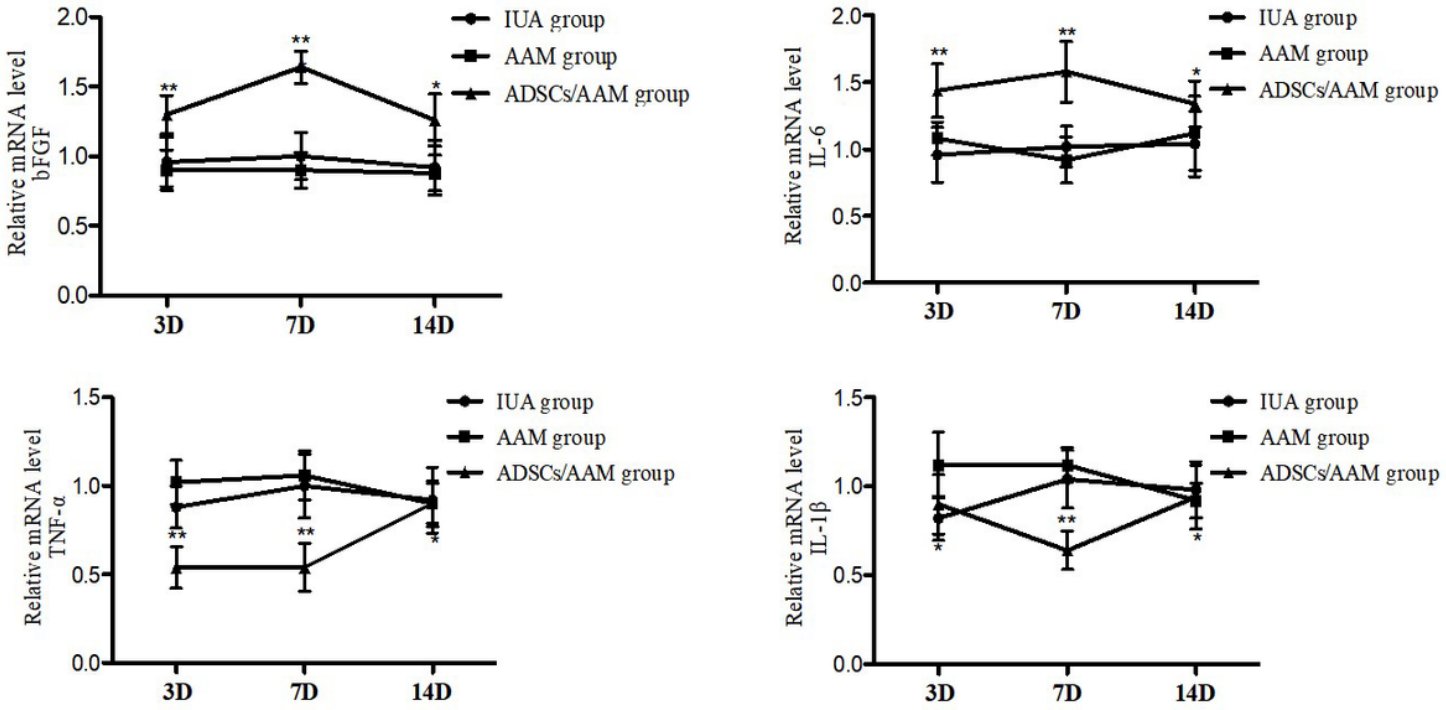

Figure 9

Tracking of ADSCs in vivo. Dil were used to show the presence of transplanted ADSCs. Green represents positive Dil staining, whereas blue color represents DAPI staining for nucleus. The merge image of the Dil and DAPI indicated the location of ADSCs in the regenerated endometrium. Scale bar = 200μm.

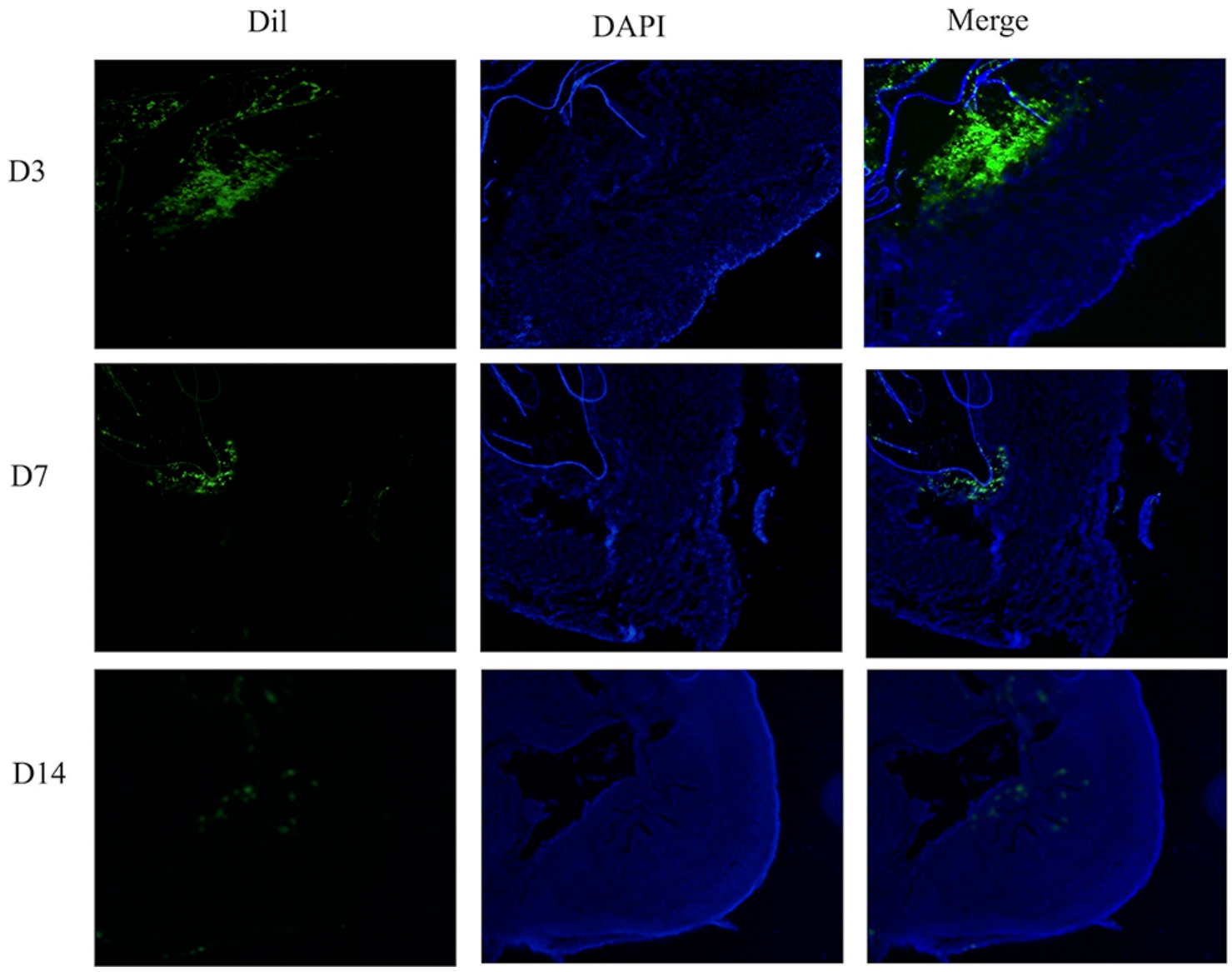

Figure 10

Legend not included with this version